J Mater Sci: Mater Electron (2016) 27:9083–9093
DOI 10.1007/s10854-016-4943-1

An investigation on the ZnO retained ratio, microstructural evolution, and mechanical properties of ZnO doped Sn3.0Ag0.5Cu composite solder joints

Hao Peng[1] · Guang Chen[1,2] · Liping Mo[1] · Y. C. Chan[3] · Fengshun Wu[1] · Hui Liu[1]

Received: 16 March 2016 / Accepted: 2 May 2016 / Published online: 6 May 2016

Abstract In this study, ZnO nanoparticles with different weight fractions (0.1, 0.25, 0.5 and 1 wt%) were successfully incorporated into Sn3.0Ag0.5Cu (SAC305) solder through powder metallurgy method. The retained ratios of ZnO reinforcements were measured, and then their effects on the thermal behaviors, microstructural evolution and mechanical properties of composite solders were systematically studied. The element content analysis revealed that only about 12 % of the initially doped ZnO nanoparticles were retained in the final solder joints. With an increase in the amount of reinforcements, the undercooling of composite solders was decreased while the melting temperature was negligibly altered. Refined β-Sn grains were obtained in the composite solder matrix after addition of ZnO nanoparticles. Moreover, compared to the plain solder joints, the composite solder joints exhibited a lower growth velocity of interfacial intermetallic compounds during isothermal aging. A 17.9 % improvement in microhardness and a 10.1 % enhancement in shear strength were also achieved for composite solder joints after 1 wt% ZnO addition. These promotions are all contributed by the presence of ZnO nanoparticles and refined microstructure in solder matrix.

✉ Fengshun Wu
fengshunwu@mail.hust.edu.cn

[1] State Key Laboratory of Materials Processing and Die & Mould Technology, Huazhong University of Science and Technology, Wuhan, China

[2] Wolfson School of Mechanical and Manufacturing Engineering, Loughborough University, Loughborough, UK

[3] Department of Electronic Engineering, City University of Hong Kong, Kowloon, Hong Kong, China

1 Introduction

During the last decades, the development of lead-free solder alloys has been considerably facilitated due to the increasing environmental and health concerns contributed by lead utilization in electronic packaging industry [1]. Among all the developed Sn-based lead-free solder alloys, Sn–Ag–Cu (SAC) solders have been acknowledged as the most attractive substitute for Sn–Pb solders owing to their relatively low cost, good solderability and superior mechanical strength [2]. Nevertheless, with the electronic packages moving towards miniaturization and high density, the conventional SAC solders were challenged by the reliability issues in smaller solder joints [3]. Therefore, novel solder alloys with better performance and higher reliability are strongly demanded for electronic interconnection.

To further promote the performance of conventional lead-free solder alloys, fabricating a composite solder alloy containing foreign reinforcements is believed to be a technically feasible and economically affordable approach. Various kinds of metals, ceramics, IMCs and carbon-based materials have been widely selected as reinforcements to synthesize composite solders [4–7]. Among different kinds of reinforcements, ceramic nanoparticles have attracted enough attention due to their relatively stable physical and chemical properties as well as their convenient access [8–11]. Tsao and Chang [8] prepared a composite SAC solder containing Al_2O_3 nanoparticles; finer microstructure was obtained in the composite solder matrix. El-Daly and Desoky [9] incorporated 0.7 wt% SiC nanoparticles into SAC305 solder; the reinforcements effectively decreased the pasty range of composite solder. Tang et al. [10] investigated the mechanical properties of SAC305-XTiO_2 composite solders; they reported that both microhardness

and tensile strength of solder alloys were improved by the existence of TiO_2 nanoparticles. Gain et al. [11] synthesized a composite SAC305 solder reinforced with ZrO_2 nanoparticles; the presence of ZrO_2 reinforcements was reported to provide a contribution to the improvement in shear strength of composite solder.

In addition to the wonderful performance in photoelectricity, some outstanding physical and chemical properties are also possessed by ZnO nanomaterials, such as high melting point (1975 °C), good thermal stability, as well as favorable elastic modulus [12]. Attempts have thus been made at synthesizing composite solders containing ZnO nanomaterials in last few years [13, 14]. Faway [13] and EI-Daly [14] studied the effect of ZnO nanoparticles on mechanical strength of SAC solders; they both reported that the yield strength (YS) and ultimate tensile strength (UTS) of composite solders were improved after ZnO nanoparticles addition. Although the effects of ZnO nanoparticles on basic properties have been preliminary investigated, the microstructural evolution as well as mechanical performance of composite solders under isothermal aging still need further study. Moreover, almost all the previously reported ZnO doped composite solders were fabricated through solder paste mixing. As stated in the literature [15], it is difficult to uniformly disperse the nano-sized reinforcements in solder matrix by simply stirring the mixed paste even for a long time. Therefore, powder metallurgic method, of which the ball milling and rolling process are believed to have positive effects on the dispersion of reinforcements, is adopted in this study to blend the reinforcements with the solder powders more efficiently. It is also worth noting that some of the ceramic reinforcements may be expelled out from the solder matrix during soldering since they can hardly be wetted by the molten solder [16]. In this case, the amount of reinforcements finally retained in the composite solders would not match with that of the reinforcements initially added. Whereas, little investigation has been conducted measuring the content of retained reinforcements in composite solders so far. Based on this motivation, in this paper, the amount of retained reinforcements (i.e. ZnO nanoparticles) in composite solders were quantitatively measured and the retained ratios were accordingly calculated. Furthermore, the effects of retained reinforcements on the microstructural evolution and mechanical properties of composite solder joints during isothermal aging were also systematically studied.

2 Materials and experimental procedures

To prepare the composite solders, SAC305 solder powders (Beijing Compo, China) and ZnO nanoparticles (Aladdin, U.S.A) were respectively used as solder matrix and reinforcements, as shown in Fig. 1a, b. The SAC305 solder powders have a particle diameter of 25–45 μm, while the ZnO nanoparticles have an average size of 30 nm. According to the X-ray diffraction (XRD) pattern shown in Fig. 1c, the ZnO nanoparticles was identified to have a wurzite crystal structure, which possesses the best thermodynamic stability over other two structures of ZnO [17].

The composite solders fabricated through powder metallurgic method were designed as SAC-XZnO (X = 0.1, 0.25, 0.5, 1) in accordance with the weight fraction (0.1, 0.25, 0.5 and 1 wt%) of ZnO nanoparticles. During preparation, a planetary mill was employed to mechanically blend the pre-weighed SAC305 solder powder and ZnO nanoparticles for 10 h with a speed of 150 r/min. After ball milling, the powder mixture was vertically compacted into a cylinder billet (Φ20 mm × 2 mm) before sintered at 180 °C for 3 h under vacuum atmosphere. The obtained solder billets were subsequently rolled at room temperature into solder foils (180 μm in thickness). For microstructure characterization and mechanical properties test, these solder foils were finally cut and reflowed into solder balls (800 μm in diameter). The plain SAC305 solder balls were fabricated through the same procedures except for the introduction of ZnO nanoparticles.

The morphology of solder powders after ball milling was observed by an environmental scanning electron microscope (ESEM, Quanta 200) with an energy dispersive X-ray spectrometer (EDX) utilized for the component analysis. To detect the reinforcements retained in solder billets and solder balls, 10 samples of each solder group were cleaned and dissolved in aqua regia before tested by an ICP-OES (Varian-720) system. The element content of Zn was measured from the solutions and the amount of retained ZnO reinforcements were calculated. A differential scanning calorimeter (DSC, PerkinElmer) was employed to study the thermal properties of composite solders. During testing, the solders were heated from 30 to 300 °C and then cooled down to 30 °C both at a rate of 10 °C/min in an inert atmosphere.

For the microstructural observation, the as-reflowed solder balls were first mounted in resin and then subjected into a mechanical grind and polish. A mixture of ethanol and hydrochloric acid (99 vol % ethanol and 1 vol % hydrochloric acid) was prepared and utilized for the etching. Afterwards, the ESEM system was used to investigate the microstructure of solder balls. To study the microstructural evolution under different isothermal aging periods, solder foils were cut and placed on a polished copper substrate before reflowing to form IMCs at the interface. Finally, the samples were put into a vacuum oven for isothermal aging; the temperature was set as 150 °C while the aging duration was set as 0, 100, 225 and 400 h, respectively. The microstructure of interfacial IMCs aged for different time was also characterized by the ESEM system.

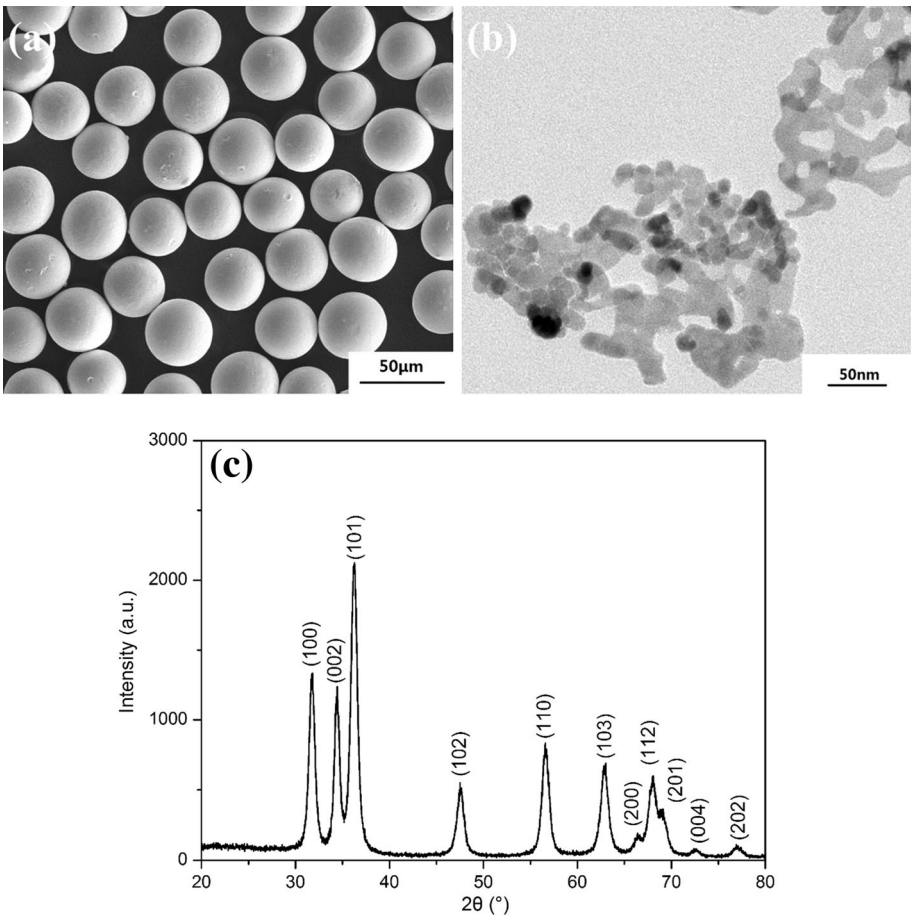

Fig. 1 **a** SEM images of SAC305 solder powders; **b** Bright field TEM images of ZnO nanoparticles; **c** XRD profiles of ZnO nanoparticles

The microhardness test was carried out through a Vickers hardness tester (MXT-CXT) at room temperature; the testing load and dwell time were respectively set as 10 g gf and 15 s. To guarantee the reliability of obtained data, thirty points of each solder were tested and the mean value was calculated. For the shear strength test, twenty solder joints formed on copper pads (600 μm in diameter) for each composite alloy were tested by a push–pull tester (DAGE 4000-plus, Nordson Co. Ltd., U.S.). The shear height and shear rate were set as 100 μm and 250 μm/s, respectively. Furthermore, to understand the fracture behaviors of solder joints, the fracture surface of solder samples after shear strength test was further investigated by the ESEM system.

3 Results and discussion

3.1 Morphology of ball-milled solder powders

The morphology of plain and composite solder powders after ball milling was shown in Fig. 2, in which the shape of SAC305 solder powders can be obviously observed to be transformed from the initial sphere (Fig. 1a) into irregular polygon. Besides, as shown in Fig. 2b, the composite solder powders have some white particles clearly on the surface in comparison to the plain solder powders.

To further understand the component of white particles, SEM observation with higher magnification and EDX analysis were carried out and presented in Fig. 3. The EDX spectrum demonstrates that these white particles are the initially added ZnO nanoparticles. Meantime, they can also be found embedded onto the surface of SAC305 solder powders, which may be related with their higher hardness than solder powders. In addition, the embedded reinforcements can be measured to have a size ranging from 150 nm to 1.5 μm. In view of the high surface energy of doped ZnO nanoparticles, these submicro particles are viewed as agglomerates of ZnO nanoparticles since they are prone to gather together with each other. This observed agglomeration also indicates that further researches are demanded to improve the dispersion of doped ceramic reinforcements on the surface of SAC305 solder powder.

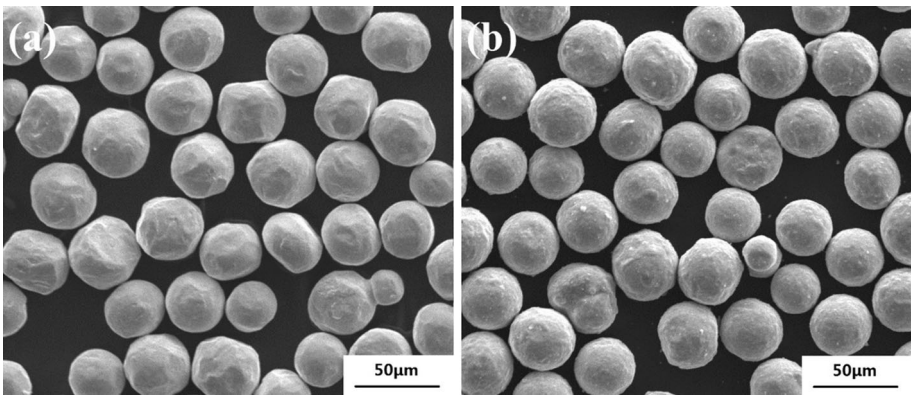

Fig. 2 The morphology of solder powders after ball milling: **a** plain solder; **b** composite solder

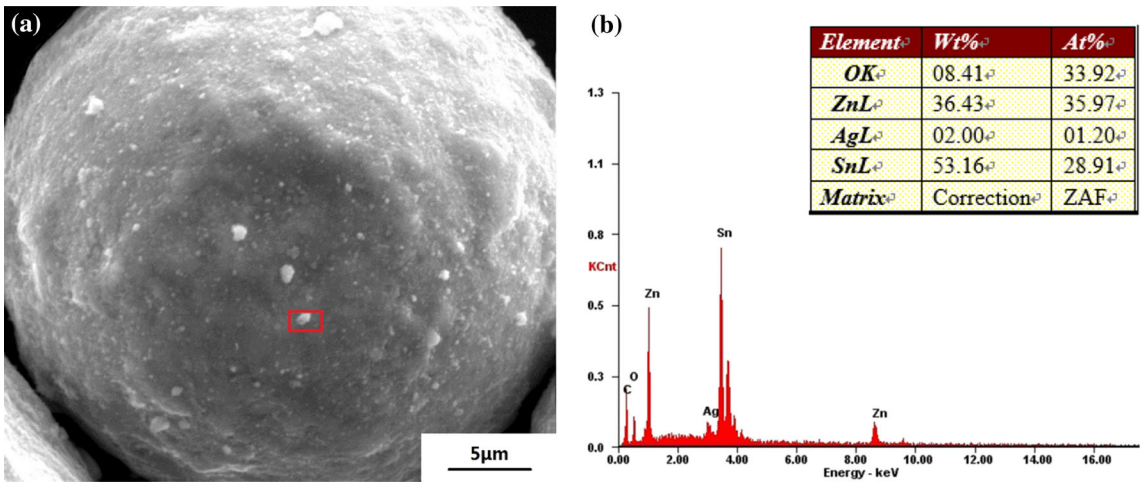

Fig. 3 **a** SEM images of ball-milled composite SAC305 solder powder with higher magnification; **b** EDX spectrum of the selected region in (**a**)

3.2 Retained ratios of ZnO nanoparticles

The measured content of retained ZnO nanoparticles in composite solders was collected in Fig. 4. A reference line, which represents the ideal conditions that all the reinforcements were retained in the solder, was also plotted in this figure. The doped reinforcements exhibited an obvious decline both in solder billets and solder joints. In detail, for the composite solders reinforced with 0.1, 0.25, 0.5 and 1 wt% ZnO nanoparticles, there are only 0.095, 0.228, 0.451, 0.815 and 0.019, 0.045, 0.082, 0.125 wt% ZnO nanoparticles retained in solder billets and solder joints, respectively.

As discussed in Fig. 3a, the ZnO nanoparticles embedded onto the surface of SAC305 solder powders successfully during ball milling. However, some ZnO nanoparticles might drop from the SAC305 powder surface as a function of the continuous collision from the grinding balls, resulting in the loss of ZnO nanoparticles in solder billets. Moreover, as a non-reacting reinforcement, ZnO nanoparticles can hardly be wetted by the molten solder during reflowing and most of them would be expelled out from the solder matrix. In such case, only a small portion (about 12 %) of the initially doped ZnO nanoparticles were retained in the finally obtained solder joints.

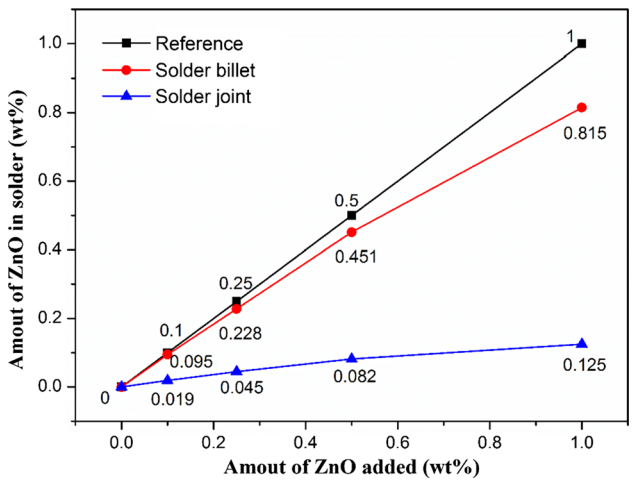

Fig. 4 The amount of ZnO nanoparticles retained in composite solder billets and solder joints

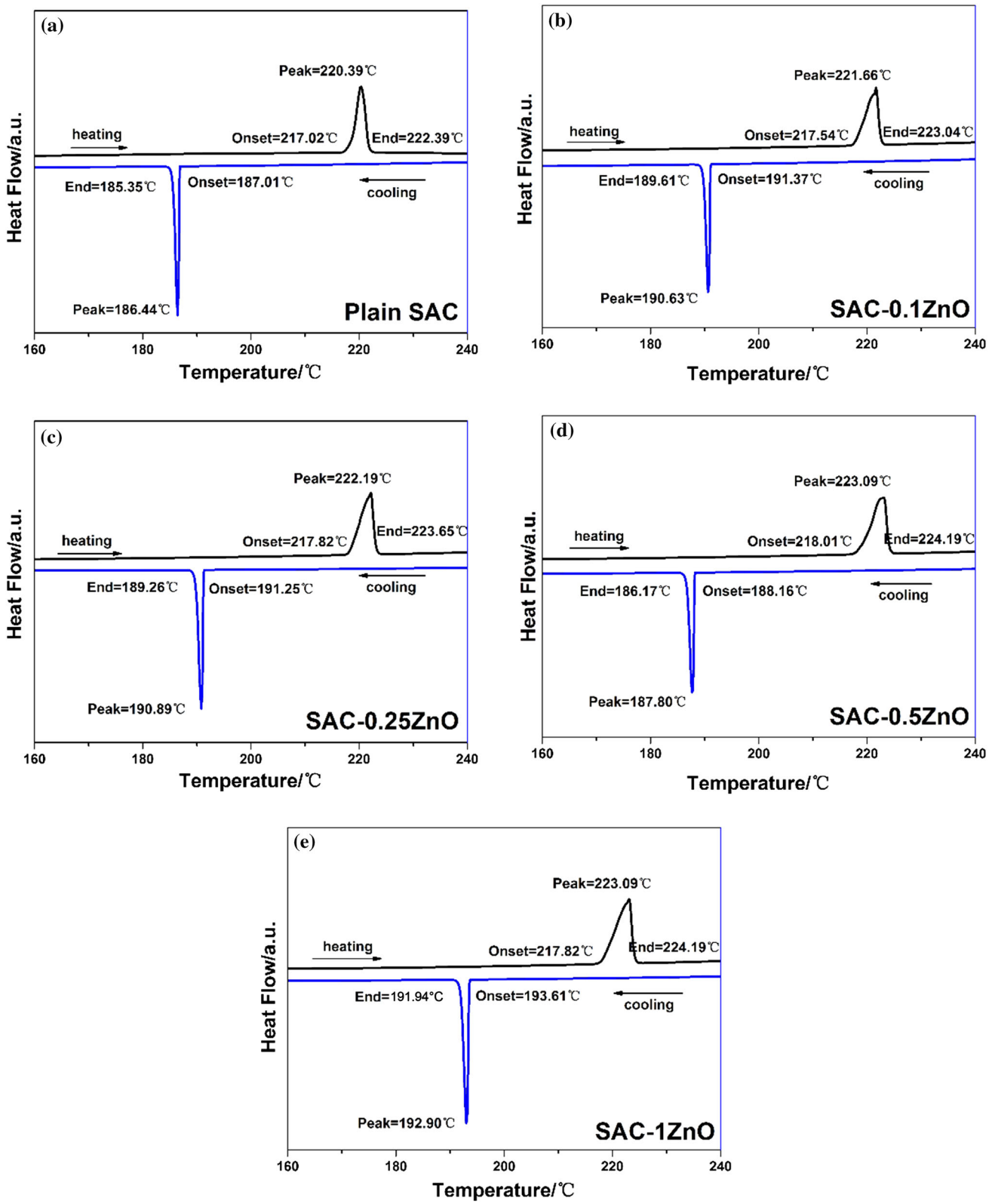

Fig. 5 DSC curves of: **a** plain SAC, **b** SAC-0.1ZnO, **c** SAC-0.25ZnO, **d** SAC-0.5ZnO and **e** SAC-1ZnO solder alloys

Table 1 Undercooling range for SAC-XZnO solder alloys from DSC curves

Sample	T_{onset} heating (°C)	T_{onset} cooling (°C)	Undercooling (°C)
SAC	217.02	187.01	30.01
SAC-0.1ZnO	217.54	191.37	26.17
SAC-0.25ZnO	217.82	191.25	26.57
SAC-0.5ZnO	218.01	188.16	29.85
SAC-1ZnO	217.82	193.61	24.21

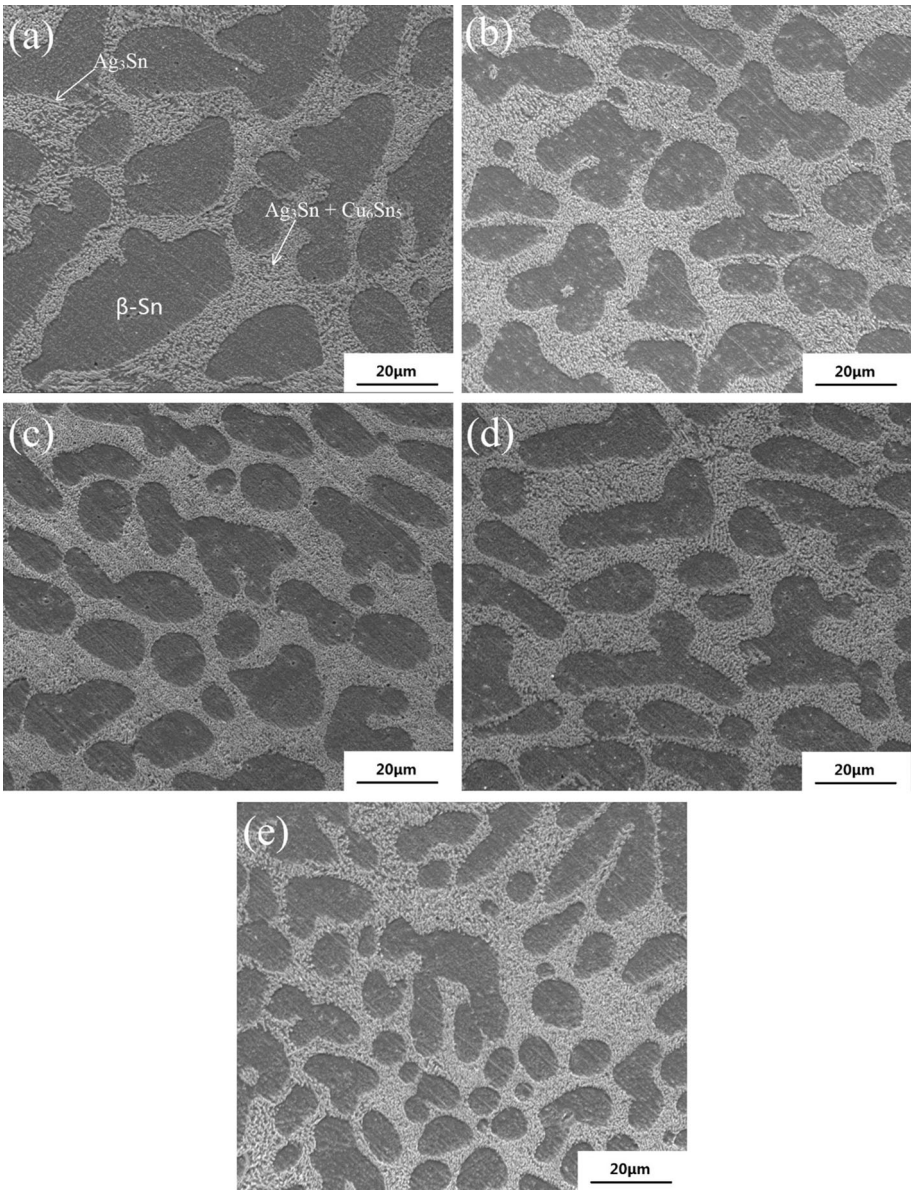

Fig. 6 Microstructure of reflowed solder: **a** SAC305; **b** SAC-0.1ZnO; **c** SAC-0.25ZnO; **d** SAC-0.5ZnO and **e** SAC-1ZnO

3.3 Thermal properties of composite solders

The DSC result of plain solder was shown in Fig. 5a, while the results of composite solders were demonstrated in Fig. 5b–e. For each solder, only a sharp endothermic peak and an exothermic peak can be observed, proving that no metallurgical reaction happened between the ZnO reinforcements and the solder matrix during heating. The onset melting temperature for five solders appeared within the range of 217.02–218.01 °C, exhibiting a change less than 1 °C. Under such case, the developed lead-free reflowing conditions can also be employed for these fabricated

Table 2 Average size of β-Sn grains in composite solder matrix

Sample#	ZnO addition (wt%)	Average size of β-Sn grains (μm)
1	Nil	23.83 ± 3.35
2	0.1	20.79 ± 2.61
3	0.25	18.16 ± 2.67
4	0.5	16.01 ± 3.08
5	1	13.76 ± 2.65

SAC305/ZnO composite solders. The tiny change in melting point for ZnO doped SAC solder was also reported in the previous study of EI-Daly [14].

Besides of the melting temperature, the undercooling of composite solders was also studied based on the DSC results. Undercooling is usually defined as the difference between the onset melting temperature during heating and the onset solidification temperature during cooling, which closely relates to the difficulty of nucleation in a liquid state [18]. Table 1 lists the undercooling values for five samples; all the composite solders exhibited a smaller undercooling than the plain solder. This phenomenon can be explained that the doped ZnO nanoparticles provided extra nucleation sites in the molten solder, leading to the promotion of solidification and giving rise to a decline in undercooling.

3.4 Microstructural evolution

3.4.1 Microstructural characterization in the solder matrix

The microstructures of reflowed plain and composite SAC305 solders were characterized and described in Fig. 6. For the plain solder, dark β-Sn grains, bright Ag_3Sn IMCs and Cu_6Sn_5 IMCs were clearly exhibited in the solder matrix. Whereas in the composite solder matrix, finer microstructure with smaller β-Sn grains was obtained after ZnO addition. To further analyze the influence of ZnO reinforcements on the microstructure of composite solders, 20 locations were randomly selected in the solder matrix to measure the size of β-Sn grains. The measured results were presented in Table 2. From the table, the average size of β-Sn grains decreased significantly with the addition of ZnO nanoparticles. The SAC-1ZnO solder possessed the finest β-Sn phase with average size of 13.76 μm, 42.3 % smaller than that in plain solder (approximately 23.83 μm). The explanation for the refinement of β-Sn grains is that the doped ZnO nanoparticles could serve as additional nucleation sites for liquid β-Sn phase during solidification, which increased the nucleation rate of β-Sn phase and restricted its growth.

3.4.2 IMC evolution at the solder/Cu interface

Though the formation of IMC layer was necessary to build a good bonding between the solder and substrate, excessive IMC would degrade the mechanical properties of solder joints due to their brittle nature [19]. Therefore, retarded IMC layer was desirable to improve the reliability of solder joints. Figure 7 characterizes the microstructural evolution of solder/Cu interface during isothermal aging. A continuous scallop-like IMC layer was produced at the as-reflowed SAC305 solder/Cu interface. After 100 h aging, a new IMC layer (Cu_3Sn) was developed between the initial IMC layer (Cu_6Sn_5) and the copper substrate. In addition, some white bulks can be observed on the surface of Cu_6Sn_5 layer and they were identified to be Ag_3Sn by means of EDX analysis.

To further study the impact of ZnO nanoparticles addition on the growth of interfacial IMCs during isothermal aging, the IMC layer's thickness after different aging periods was quantitatively measured and plotted in Fig. 8. Usually, the growth of IMC can be expressed by the following growth equation:

$$D = D_0 + Kt^n \quad (1)$$

where D is the thickness of interfacial IMC layer; D_0 is the initial thickness of interfacial IMC layer after reflowing; K is the growth velocity of IMC; t represents the aging time; n stands for the growth index, which relates to the growth patterns of IMC between solder and substrate. Under the conditions of isothermal aging, the growth of IMC is believed to be mainly determined by the element diffusion and the growth index n is set as 0.5 [20]. The novel growth equation can be described as follows:

$$D - D_0 = K\sqrt{t} \quad (2)$$

The curves representing the relationship of interfacial IMC thickness with the square root of the aging time was plotted in Fig. 9. Then the growth velocity of IMC layer (K) was calculated and presented in Fig. 10. From the figure, the growth velocity (K) of interfacial IMC layer in plain solder joints can be calculated as 3.88×10^{-3} μm/s$^{1/2}$. After 1 wt% ZnO nanoparticles addition, the growth velocity (K) showed an 18.6 % decline to 3.16×10^{-3} μm/s$^{1/2}$. It can be concluded that the addition of ZnO nanoparticles effectively impeded the growth of interfacial IMC layer during isothermal aging. The impeding effect can be ascribed to the doped ZnO reinforcements and refined β-Sn grains in the solder matrix. These particles could serve as a

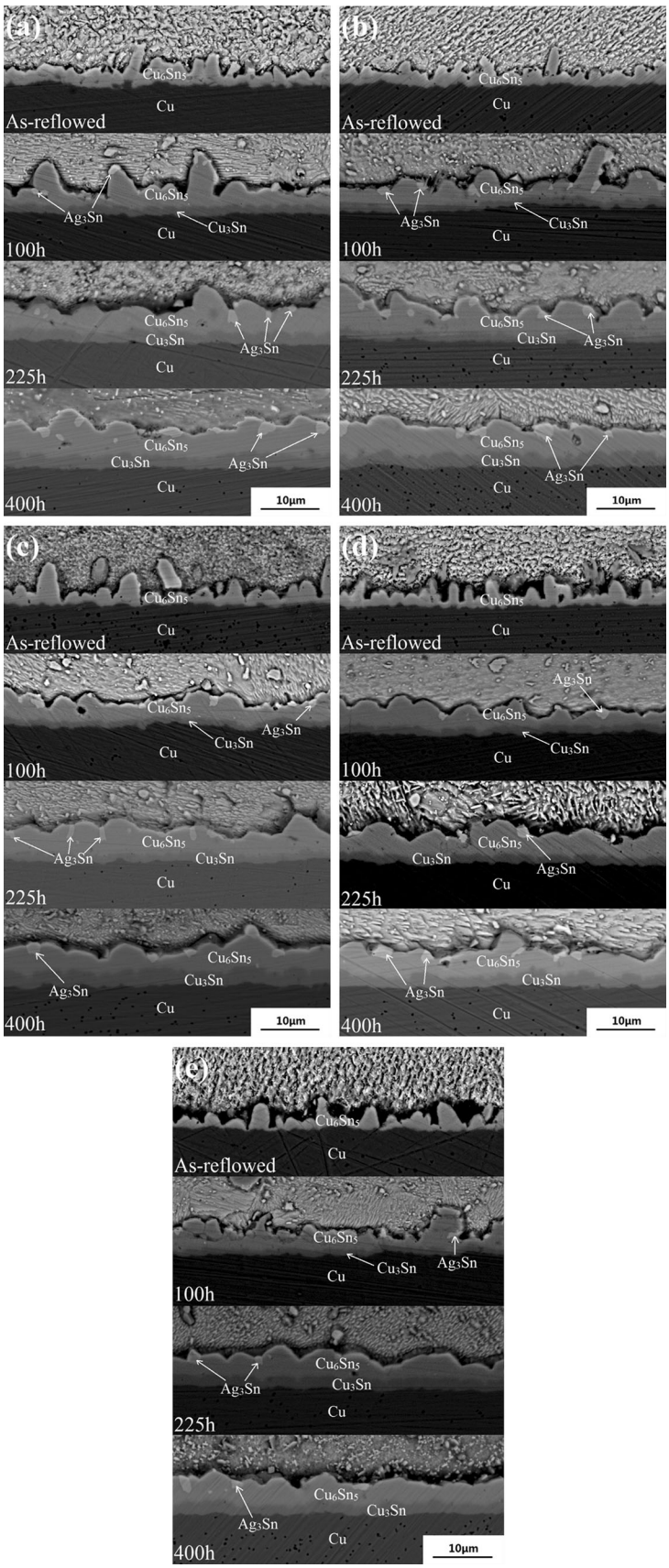

Fig. 7 The microstructure of IMC layers at SAC-XZnO solder/Cu interface under 150 °C isothermal aging for 0, 100, 225 and 400 h (**a** X = 0; b: X = 0.1; c: X = 0.25; d: X = 0.5; e: X = 1)

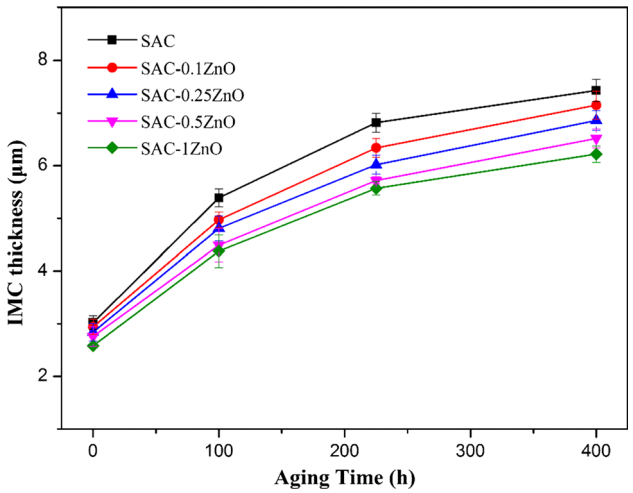

Fig. 8 The thickness of IMC layer at solder/Cu interface for different aging time

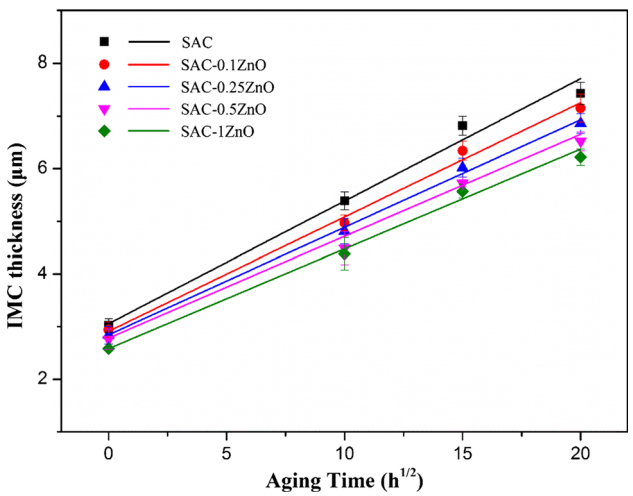

Fig. 9 Linear relationship between the IMC thickness and the square root of aging time

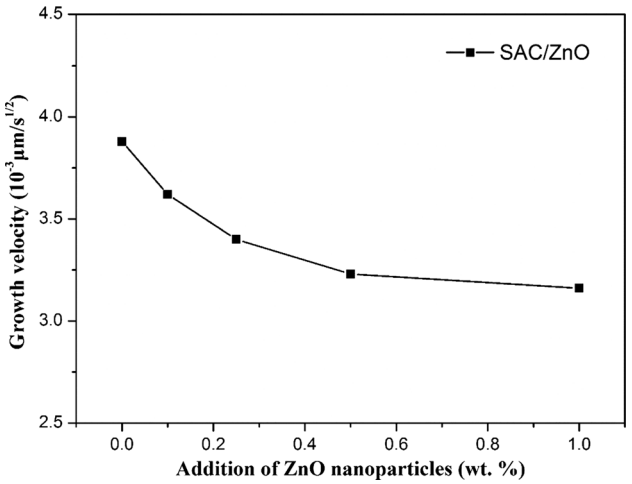

Fig. 10 Growth velocity of interfacial IMC layer in plain and composite solder joints

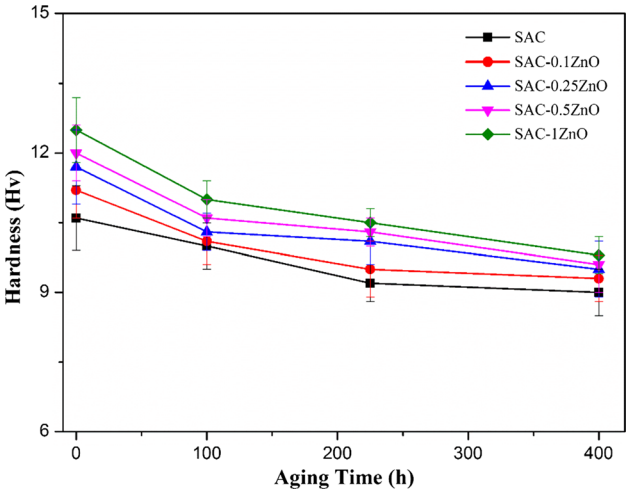

Fig. 11 Microhardness of plain and composite solder joints after different time aging

barrier to retard the diffusion of Sn and Cu atoms, thus hindering the growth of IMC layer during isothermal aging.

3.5 Mechanical properties

3.5.1 Microhardness

Microhardness is usually used to evaluate the mechanical properties of solders since this factor offers a reference of resistance to abrasion and deformation [21]. Figure 11 demonstrates the microhardness values of five solders after different isothermal aging periods. The microhardness increased with the addition of ZnO nanoparticles while decreased with the aging time. After reflowing, the SAC-1ZnO possessed the maximum microhardness of 12.5 Hv, which was 17.9 % higher than that of plain solder. After aged for 400 h, the microhardness of SAC-1ZnO composite solder still outperformed (8.9 % higher) plain solder even though it showed a decline to 9.8 Hv.

The refined β-Sn grains shown in Fig. 6 can help to explain the improvement in microhardness due to the substantial effects of microstructure on the mechanical properties of solder alloys [23]. Moreover, according to the dispersion strengthening theory, the foreign ZnO reinforcements located in the solder matrices and grain boundaries would restrict the movement of dislocation and hinder the grain boundaries sliding, leading to the improvement in microhardness as well [24].

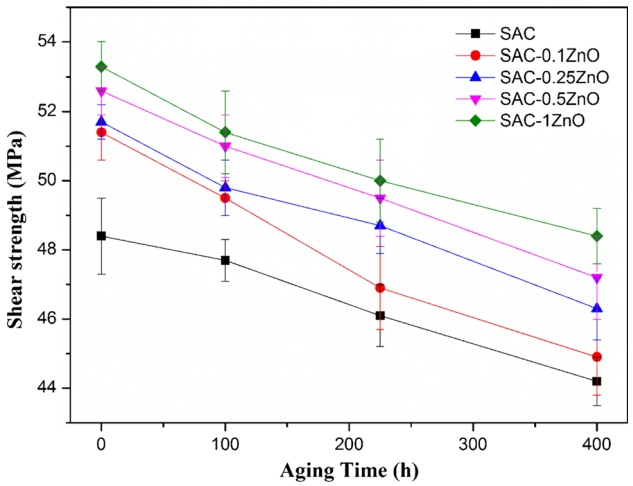

Fig. 12 Shear strength of plain and composite solder joints after different time aging

3.5.2 Shear strength

Shear strength is another extensively accepted parameter of mechanical properties associated with the reliability of solders. During service periods, the mechanical loading is often applied on the solder joints, and thus favorable shear strength is of critical importance for solder joints to guarantee the reliability of electric devices [22]. The shear strength values of aged solder joints were collected in Fig. 12. The addition of ZnO nanoparticles improved the shear strength of solder joints while the isothermal aging had a negative impact. After 1 wt% ZnO nanoparticles were added, the shear strength of non-aged SAC305 solder increased 10.1 % from 48.4 to 53.3 MPa. Furthermore, all the composite solders performed better than plain solder in shear strength throughout the isothermal aging periods. Particularly, the SAC-1ZnO composite solder joints had the shear strength of 51.4, 50.0 and 48.4 MPa after aging for 100, 225, and 400 h, which was 7.8, 8.5 and 9.5 % higher than that of plain solder, respectively. As in the analysis of microhardness, the improvement in shear strength can also be ascribed to the presence of ZnO nanoparticles and refined microstructure in the solder matrix.

After shear strength test, the fracture surfaces of solder joints were further observed by ESEM. As shown in Fig. 13a, b, a surface containing a relatively smooth region and a rough dimple region could be observed for the plain solder. After addition of ZnO nanoparticles, the composite solder joints exhibited a fracture surface with the same composition. Both the plain and composite SAC305 solders exhibited a ductile fracture mode. In other words, the addition of ZnO nanoparticles is believed to have insignificant impact on the fracture behavior of solder joints, which may relates to the little retained amount of reinforcements in the composite solder.

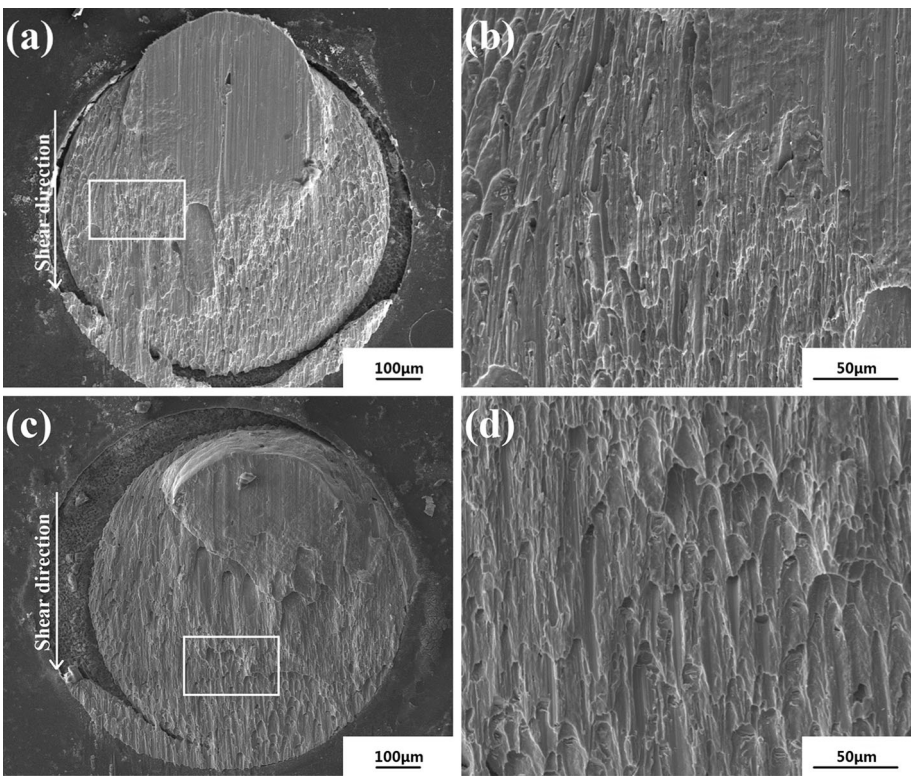

Fig. 13 Fractured surfaces of SAC305 (**a**, **b**) and SAC-1ZnO (**c**, **d**) solder joints after shear strength test

4 Conclusions

In this study, ZnO doped SAC305 composite solders were successfully fabricated through the powder metallurgy method. After ball milling, the added ZnO nanoparticles embedded onto the surface of SAC305 solder powders and some of them aggregated into agglomerates. A considerable loss occurred to the ZnO reinforcements both in solder billets and solder joints; the reason is that they would drop from the surface of solder powders during ball milling and be excluded from the solder matrix during reflowing. After addition of ZnO nanoparticles, the composite solders witnessed a reduced undercooling while maintained an approximately constant melting temperature. Finer microstructure with smaller β-Sn grains was achieved in the composite solder matrix. Furthermore, due to the presence of ZnO reinforcements and refined microstructure, the growth of IMC layer at solder/Cu interface was impeded, and the mechanical properties of composite solders were improved though the fracture mode was not significantly altered.

Acknowledgments The authors would like to acknowledge the research funding by National Nature Science Foundation of China (NSFC) and Research Grants Council (RGC) Joint Research project (NSFC No. 61261160498, RGC No. CityU101/12). Thanks are also given to the State Key Laboratory of Materials processing and Die & Mould Technology as well as the Analytical and Testing Center in Huazhong University of Science and Technology (HUST) for the analytical and testing services.

References

1. H.R. Kotadia, P.D. Howes, S.H. Mannan, A review: on the development of low melting temperature Pb-free solders. Microelectron. Reliab. **54**, 1253–1273 (2014)
2. D.Q. Yu, L. Wang, The growth and roughness evolution of intermetallic compounds of Sn–Ag–Cu/Cu interface during soldering reaction. J. Alloys. Compd. **458**, 542–547 (2008)
3. I.E. Anderson, Development of Sn–Ag–Cu and Sn–Ag–Cu–X alloys for Pb-free electronic solder applications. J. Mater. Sci.: Mater. Electron. **18**, 55–76 (2007)
4. A. Nadia, A.S.M.A. Haseeb, Effects of addition of copper particles of different size to Sn–3.5Ag solder. J. Mater. Sci.: Mater. Electron. **23**, 86–93 (2012)
5. L.C. Tsao, C.H. Huang, C.H. Chung, R.S. Chen, Influence of TiO_2 nanoparticles addition on the microstructural and mechanical properties of Sn0.7Cu nano-composite solder. Mater. Sci. Eng. A **545**, 194–200 (2012)
6. S.T. Kao, Y.C. Lin, J.G. Duh, Controlling intermetallic compound growth in SnAgCu/Ni-P solder joints by nanosized Cu6Sn5 addition. J. Electron. Mater. **35**, 486–493 (2006)
7. K.M. Kumar, V. Kripesh, L. Shen, Study on the microstructure and mechanical properties of a novel SWCNT-reinforced solder alloy for ultra-fine pitch applications. Thin Solid Films **504**, 371–378 (2006)
8. L.C. Tsao, S.Y. Chang, Effects of nano-Al_2O_3 additions on microstructure development and hardness of Sn3.5Ag0.5Cu solder. Mater. Des. **31**, 4831–4835 (2010)
9. A.A. El-Daly, W.M. Desoky, Microstructural modifications and properties of SiC nanoparticles-reinforced Sn–3.0Ag–0.5Cu solder alloy. Mater. Des. **65**, 1196–1204 (2015)
10. Y. Tang, G.Y. Li, Y.C. Pan, Effects of TiO_2 nanoparticles addition on microstructure, microhardness and tensile properties of Sn–3.0Ag–0.5Cu–xTiO_2 composite solder. Mater. Des. **55**, 574–582 (2014)
11. A.K. Gain, Y.C. Chan, W.K.C. Yung, Effect of additions of ZrO_2 nano-particles on the microstructure and shear strength of Sn–Ag–Cu solder on Au/Ni metallized Cu pads. Microelectron. Reliab. **51**, 2306–2313 (2011)
12. A.K. Swarnakar, L. Donze, J. Vleugels, High temperature properties of ZnO ceramics studied by the impulse excitation technique. J. Eur. Ceram. Soc. **29**, 2991–2998 (2009)
13. A. Fawzy, S.A. Fayek, Tensile creep characteristics of Sn–3.5Ag–0.5Cu (SAC355) solder reinforced with nano-metric ZnO particles. Mater. Sci. Eng. A **603**, 1–10 (2014)
14. A.A. El-Daly, T.A. Elmosalami, Tensile deformation behavior and melting property of nano-sized ZnO particles reinforced Sn–3.0Ag–0.5Cu lead-free solder. Mater. Sci. Eng. A **618**, 389–397 (2014)
15. Y. Shi, J. Liu, Y. Yan, Creep properties of composite solders reinforced with nano-and microsized particles. J. Electron. Mater. **37**, 507–514 (2008)
16. J. Shen, Y.C. Chan, Research advances in nano-composite solders. Microelectron. Reliab. **49**, 223–234 (2009)
17. E. Grzanka, S. Gierlotka, S. Stelmakh, Phase transition in nanocrystalline ZnO. Z Kristallogr Suppl. **23**, 337–342 (2006)
18. A.A. El-Daly, G.S. Al-Ganainy, A. Fawzy, Structural characterization and creep resistance of nano-silicon carbide reinforced Sn–1.0Ag–0.5Cu lead-free solder alloy. Mater. Des. **55**, 837–845 (2014)
19. L.C. Tsao, Suppressing effect of 0.5 wt% nano-TiO2 addition into Sn–3.5Ag–0.5Cu solder alloy on the intermetallic growth with Cu substrate during isothermal aging. J. Alloys Compd. **509**, 8441–8448 (2011)
20. L. Xu, J.H.L. Pang, K.H. Prakash, Isothermal and thermal cycling aging on IMC growth rate in lead-free and lead-based solder interface. IEEE T. Compon. Pack. T. **28**, 408–414 (2005)
21. M. Ahmed, T. Fouzder, A. Sharif, Influence of Ag micro-particle additions on the microstructure, hardness and tensile properties of Sn–9Zn binary eutectic solder alloy. Microelectron. Reliab. **50**, 1134–1141 (2010)
22. J. Shen, Y.C. Chan, Effects of ZrO_2 nanoparticles on the mechanical properties of Sn–Zn solder joints on Au/Ni/Cu pads. J. Alloys. Compd. **477**, 552–559 (2009)
23. G. Chen, F. Wu, C. Liu, Effects of fullerenes reinforcement on the performance of 96.5Sn–3Ag–0.5Cu lead-free solder. Mater. Sci. Eng. A **636**, 484–492 (2015)
24. L.C. Tsao, S.Y. Chang, Effects of nano-TiO_2 additions on thermal analysis, microstructure and tensile properties of Sn3.5Ag0.25Cu solder. Mater. Des. **31**, 990–993 (2010)